Available online at www.sciencedirect.com
ScienceDirect
Journal of Molecular Catalysis A: Chemical 263 (2007) 149–155
JOURNAL OF MOLECULAR CATALYSIS A: CHEMICAL
www.elsevier.com/locate/molcata

$MnCl_2$ modified $H_4SiW_{12}O_{40}/SiO_2$ catalysts for catalytic oxidation of dimethy ether to dimethoxymethane

Qingde Zhang [a,b], Yisheng Tan [a], Caihong Yang [a], Yizhuo Han [a,*]

[a] *State Key Laboratory of Coal Conversion, Institute of Coal Chemistry, Chinese Academy of Sciences, Taiyuan 030001, PR China*
[b] *Graduate University of Chinese Academy of Sciences, Beijing 100039, PR China*

Received 19 June 2006; received in revised form 4 August 2006; accepted 8 August 2006
Available online 24 August 2006

Abstract

The catalytic oxidation of dimethy ether (DME) to dimethoxymethane (DMM) was carried out over $MnCl_2$ modified $H_4SiW_{12}O_{40}/SiO_2$ catalysts prepared by impregnation method in a continuous flow type fixed-bed reactor with ratio of $n_{DME}/n_{O_2} = 1:1$ at 593 K and 0.1 MPa. The effect of calcination temperatures, different impregnation sequences, reaction time and different feeding modes over $MnCl_2$(5 wt%)–$H_4SiW_{12}O_{40}/SiO_2$ catalyst were all investigated. The results show that the catalyst, which was prepared by first $H_4SiW_{12}O_{40}$ then $MnCl_2$ impregnated in SiO_2 and calcined at 673 K demonstrates the optimum activity with 8.6% of DME conversion and 39.1% of DMM selectivity. The pure DME reactants form higher selectivity of DMM than pure CH_3OH reactants. The BET surface area, total pore volume, X-ray diffraction (XRD), NH_3-TPD, TEM, FT-IR, XPS and ICP-AES were used to characterize the structure and performance of the catalysts deeply. XPS shows that Mn^{4+} species of the fresh catalyst play important role and may be reduced to Mn^{2+} or Mn^{3+} species in the synthesis of DMM from DME oxidation reaction. Besides, the amount of superficial Mn declines by 15.5% after the reaction. ICP-AES indicates that the total amount of Mn after the reaction decreases by only 4.9% than that of the fresh sample. XRD patterns of the catalysts calcined at different temperatures show that the Keggin structure of the catalysts are destroyed when the temperature exceeds 673 K, Besides, NH_3-TPD profiles also indicate that the acidity of the catalyst becomes weaker with the calcination temperature increased. Compared to the fresh catalyst, the acidity of the catalyst after the reaction is also weakened. It is found that Mn modified $H_4SiW_{12}O_{40}/SiO_2$ improves the catalyst oxidative activity and moderates the acidity of the catalyst. The mechanism of this reaction may be that DMM can be synthesized via methoxy groups formed by DME dissociation under the cooperation of the acid sites and redox sites of Mn modified $H_4SiW_{12}O_{40}/SiO_2$ catalysts.

Keywords: $MnCl_2$ modified $H_4SiW_{12}O_{40}/SiO_2$; Catalytic oxidation; Dimethy ether; Dimethoxymethane; XRD; NH_3-TPD; TEM; FT-IR; XPS; ICP-AES

1. Introduction

Dimethoxymethane (DMM, $CH_3OCH_2OCH_3$), as an important chemical material, has been widely used. It can be used as a solvent in the perfume industry, a key intermediate for preparing high-concentration formaldehyde [1], and a reagent in organic synthesis. More importantly, DMM, with high content of oxygen and cetane number, which can improve diesel oil thermal efficiency, is considered to be an extraordinarily promising additive to diesel oil [2]. Besides, as a product for environmental protection, it can substitute Freon and reduce the emission of VOCs especially.

At present, DMM can be produced by acetalization of methanol with formaldehyde in a large scale [3]. There also exist other synthesis routes, such as the direct synthesis from synthesis gas [4] via CO hydrogenation and the selective oxidation of methanol [5,6]. Liu and Iglesia have reported their research work on the synthesis of DMM from DME and methanol in a microreactor using $H_{3+n}V_nMo_{12-n}PO_{40}$ as the catalyst [7], and gets the 1.8% of DME conversion and 56.8% of DMM selectivity on $H_5PV_2Mo_{10}O_{40}$ catalyst.

DME is a potential chemical feedstock like methanol. When it is produced at big scale, the production cost will be much lower than methanol based on methyl or methoxy which are the basic group for further organic synthesis. Using DME as the starting material to synthesize a variety of organic compounds with high value will be as important as using methanol.

In our previous work, we have made some research on how to synthesize DMM via the catalytic oxidation of DME over Mn modified $H_4SiW_{12}O_{40}$ catalysts [8].

* Corresponding author. Tel.: +86 351 4049747; fax: +86 351 4044287.
E-mail address: hanyz@sxicc.ac.cn (Y. Han).

1381-1169/$ – see front matter © 2006 Elsevier B.V. All rights reserved.
doi:10.1016/j.molcata.2006.08.044

In this study, we report the catalytic activity and characterization of $MnCl_2$ modified $H_4SiW_{12}O_{40}/SiO_2$ catalysts for catalytic oxidation of DME to DMM, discuss the deactivation of the catalyst and propose the reaction mechanism.

2. Experimental

2.1. Catalyst preparation

$MnCl_2$ modified $H_4SiW_{12}O_{40}$ catalysts were prepared by an incipient wetness impregnation method. An aqueous solution of $H_4SiW_{12}O_{40}$ (Shanghai Chemical Co.) and an aqueous solution of $MnCl_2$ (Tianjin Chemical Co.) were all together impregnated in SiO_2 (Shanghai Chemical Co. 20–40 mesh) at 298 K for 4 h, then was dried in air at 393 K for 12 h, and then calcined for 4 h at 673 K. The catalyst prepared was designated as $(MnCl_2(5\ wt\%) + H_4SiW_{12}O_{40})/SiO_2$.

Two-step impregnation method: when the impregnation sequence was that first $H_4SiW_{12}O_{40}$ was impregnated in SiO_2, dried and calcined, then $MnCl_2$ was impregnated in the above sample, $MnCl_2(5\ wt\%)$–$H_4SiW_{12}O_{40}/SiO_2$ was prepared, while the catalyst prepared by the opposite sequence was designated as $H_4SiW_{12}O_{40}$–$MnCl_2(5\ wt\%)/SiO_2$.

2.2. Dimethy ether catalytic oxidation

The catalytic oxidation reactions were carried out in a continuous flow type fixed-bed reactor containing catalyst (4.8–5.0 g, 20–40 mesh) diluted with ground quartz in order to prevent over-heating of the catalyst due to the exothermic reaction. The catalyst was treated in flow of O_2 (15 ml/min) for 1 h before reaction. The reactant mixture consisted of DME and O_2 with ratio of $n_{DME}/n_{O_2} = 1:1$. The outlet stream line from the reactor to the gas chromatograph was heated at 423 K. The reaction products were analyzed by on-line gas chromatography (GC-9A) equipped with Porapak T column and GC-4000A with TDX-01 column with thermal conductivity detectors. The products selectivity are calculated on carbon molar base: $S_i = Y_i n_i / \sum Y_i n_i \times 100\%$, where i is the $CH_3OCH_2OCH_3$, CH_3OH, HCHO, $HCOOCH_3$, CH_2CH_2, CO, CO_2, CH_4, S_i the selectivity of product i, Y_i the number of carbon atom of product i, and n_i is the molar of product i.

The carbon balance of the reaction:

$$C(\text{mol}\%) = C_{\text{mol,out}}/C_{\text{mol, in}} = (2n_{\text{u,DME}} + 3n_{CH_3OCH_2OCH_3} + n_{CH_3OH} + n_{HCHO} + 2n_{HCOOCH_3} + 2n_{CH_2CH_2} + n_{CO} + n_{CO_2} + n_{CH_4})/2n_{\text{o,DME}}$$

Most of the carbon balances of the experiments are within the range of 95–99%.

2.3. Catalyst characterization

Surface areas of the samples were measured by a BET nitrogen adsorption method at 77.35 K using a TriStar 3000 machine. Total pore volume was measured by single point adsorption.

XRD patterns were measured on a Bruker Advanced X-Ray Solutions/D8-Advance using Cu Ka radiation. The anode was operated at 40 kV and 40 mA. The 2θ angles were scanned from 5° to 70°.

FT-IR spectra were measured on a NICOLET 380 instrument with a DTGS KBr detector.

XPS spectra were measured on a XPS-AXIS Ultra of Kratos Co. by using Mg Kα radiation ($h\upsilon = 1253.6$ eV) with X-ray power of 225 W (15 kV, 15 mA).

TEM images were taken on a H-600-2 Transmission electron microscope.

ICP-AES—Atomscan 16 of American TJA Co. was used to detect the total amount of Mn before and after reaction.

The NH_3-TPD spectra were recorded in a fixed-bed reactor system equipped with a gas chromatograph. The catalyst (100 mg) was pretreated at 773 K under Ar flow (40 ml/min) for 2 h and then cooled to 373 K under Ar flow. Then NH_3 was introduced into the flow system. The TPD spectra were recorded at a temperature rising rate of 10 K/min from 373 to 1273 K.

3. Results and discussion

3.1. Effects of calcination temperature on the catalytic performance of $MnCl_2(5\ wt\%)$–$H_4SiW_{12}O_{40}/SiO_2$

Table 1 shows the DME conversion, DMM and other side-products selectivities obtained over $MnCl_2(5\ wt\%)$–$H_4SiW_{12}O_{40}/SiO_2$ catalyst calcined at different temperatures. When $MnCl_2(5\ wt\%)$–$H_4SiW_{12}O_{40}/SiO_2$ sample was calcined at 623 K, DME conversion reaches 13% and 18.6% selectivity of DMM is also observed, but selectivities of side-products CO and CO_2 are given at 16.4% and 19.4%, respectively. When the sample was treated at 673 K, the DMM selectivity is significantly improved up to 39.1% with 8.6% conversion of DME. Besides $(CO + CO_2)$ selectivity obviously declines to 6.6%. However, with calcination temperature increases, DMM selectivity decreases in evidence, concurrently CO_x and CH_3OH selectivities increase sharply. Especially, CH_3OH is the main

Table 1
Comparison of the catalytic activity of $MnCl_2(5\ wt\%)$–$H_4SiW_{12}O_{40}/SiO_2$ catalyst calcined at different temperatures

Calcination temperature (K)	DME conversion (%)	Selectivity (mol%)						
		DMM	HCHO	MF	CH_3OH	C_2H_4	CO	CO_2
623	13	18.6	3.0	10.4	29.8	2.4	16.4	19.4
673	8.6	39.1	8.5	9.3	33	3.6	3.2	3.4
723	9.1	10.1	7.1	12.5	49.8	3.6	7.0	9.9
823	6.5	5.9	10.8	12.1	46.8	4.9	4.8	14.7

$T = 593$ K; $P = 0.1$ MPa; $t = 30$ min; SV = 360 h^{-1}.

Table 2
Structure properties of $MnCl_2$(5 wt%)–$H_4SiW_{12}O_{40}/SiO_2$ catalysts calcined at different temperatures

	623 K	673 K	723 K	823 K
BET surface area, A ($m^2\ g^{-1}$)	178.1	192.9	191.8	172.1
Total pore volume, v ($cm^3\ g^{-1}$)	0.132	0.147	0.148	0.146
Average pore diameter, d (nm)	2.975	3.042	3.101	3.390

$d = 4v/A$.

side-product when temperature exceeded 673 K. As can be seen from the above table, the optimum calcined temperature is 673 K with relatively high DMM selectivity and low CO_x selectivity.

Table 2 lists the surface area, average pore diameter and total pore volume of $MnCl_2$(5 wt%)–$H_4SiW_{12}O_{40}/SiO_2$ catalysts calcined at different temperatures. BET surface area of the sample calcined at 673 K reaches the highest, and its total pore volume is also relatively larger. This could explain partly why the sample calcined at 673 K exhibits the better catalytic activity in accordance with the results shown in Table 1. Then with the calcination temperatures increased, BET surface area and total pore volume of the sample show the downtrend, which can account for part of surface sintering of the catalyst. This may be one of the reasons that lead to the drop of activity and stability of the sample. Comparatively, high BET surface area, as one of the factors, helps to increase the activity of the sample and promotes the DMM synthesis from the oxidation of DME.

3.2. Influence of the impregnation sequence of $MnCl_2$ introduction into $H_4SiW_{12}O_{40}/SiO_2$ on performance of catalysts

Table 3 demonstrates the influence of the sequence of procedure in preparing $MnCl_2$(5 wt%)–$H_4SiW_{12}O_{40}/SiO_2$ catalyst. Obviously Mn modified $H_4SiW_{12}O_{40}/SiO_2$ catalysts obtain much higher DMM selectivity than $H_4SiW_{12}O_{40}$(40%)/SiO_2. Some distinctive differences of the product selectivity are displayed in Table 3. $H_4SiW_{12}O_{40}$–$MnCl_2$(5 wt%)/SiO_2 catalyst gives higher DME conversion, but DMM selectivity is relatively lower. Besides, CO_x selectivity reaches 29.2%, especially CO_2 selectivity achieves 21.4%, which is much higher than that of the other two catalysts. Maybe the acidity of $H_4SiW_{12}O_{40}$–$MnCl_2$(5 wt%)/SiO_2 catalyst is stronger so that DME was adsorbed on the catalyst and deeply oxidized to CO_2.

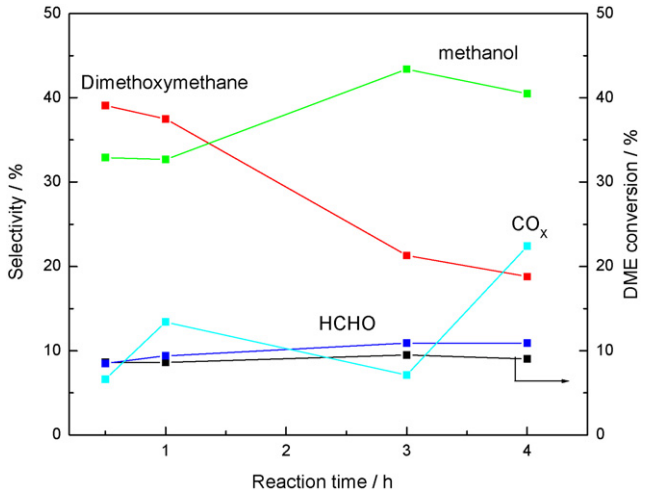

Fig. 1. Effects of reaction time on DME conversion and DMM selectivity over $MnCl_2$(5 wt%)–$H_4SiW_{12}O_{40}/SiO_2$ catalyst, T = 593 K, P = 0.1 MPa.

It is found that DMM selectivity is improved up to 39.1% and to a concurrent decrease in CO_x selectivity when the sequence of the adding $MnCl_2$ and $H_4SiW_{12}O_{40}$, respectively, was converted first $H_4SiW_{12}O_{40}$ then $MnCl_2$. Obviously, high CH_3OH selectivity is also obtained at the same time comparing to the other catalysts though ($MnCl_2$(5 wt%) + $H_4SiW_{12}O_{40}$)/SiO_2 catalyst gives 33.1% DMM selectivity. From Table 3, it is found that Mn modification greatly improves the catalytic activity of $H_4SiW_{12}O_{40}/SiO_2$ and the catalyst prepared by the Mn-acid sequence ($MnCl_2$(5 wt%)–$H_4SiW_{12}O_{40}/SiO_2$) shows best catalytic performance.

3.3. Influence of reaction time on DME conversion and DMM selectivity on $MnCl_2$(5 wt%)–$H_4SiW_{12}O_{40}/SiO_2$ catalyst

Fig. 1 shows the effects of reaction time on the conversion of DME and the selectivities of the main products over $MnCl_2$(5 wt%)–$H_4SiW_{12}O_{40}/SiO_2$ catalyst. It can be seen that the conversion of DME has no obvious change, but the selectivity of DMM decreases from 39.1% to 18.8% with the time on stream. Before 3 h, CO_x selectivity first increases then declines, and there is a concurrent increase in CH_3OH selectivity. After that, CH_3OH and DMM selectivities both decrease while CO_x selectivity rises in evidence. With the reaction time going on, DME is mostly oxidized to CO_x. It can be found that Mn

Table 3
Effect of impregnation sequences on performance of catalysts

Sequences	DME conversion (%)	Selectivity (mol%)							
		DMM	HCHO	MF	CH_3OH	C_2H_4	CO	CO_2	CH_4
$H_4SiW_{12}O_{40}$(40%)/SiO_2	21.5	5.5	8.5	6.1	41.8	2.0	28.9	6.3	0.9
$H_4SiW_{12}O_{40}$–$MnCl_2$(5 wt%)/SiO_2	10.1	16	8.3	4.1	39.2	3.1	7.8	21.4	0
$MnCl_2$(5 wt%)–$H_4SiW_{12}O_{40}/SiO_2$	8.6	39.1	8.5	9.3	33	3.6	3.2	3.4	0
($MnCl_2$(5 wt%) + $H_4SiW_{12}O_{40}$)/SiO_2	9.3	33.1	6.4	9.5	42.4	3.4	3.4	1.8	0

T = 593K; P = 0.1 MPa; t = 30 min; SV = 360 h^{-1}.

Table 4
Effect of feeding modes on performance of catalysts

Reactant	DME (or CH_3OH) conversion (%)	Selectivity (%)						
		DMM	HCHO	MF	CH_3OH (DME)	C_2H_4	CO	CO_2
DME	6.3	37.5	9.4	3.6	32.7	3.4	6.5	6.9
CH_3OH	68.4	3.9	2.5	0.8	61.3	11.9	12.4	7.2
DME + H_2O	38.9	0	1.5	0	82.1	0.3	0	16.1

$T = 593$ K; $P = 0.1$ MPa; $t = 1$ h.

modification greatly improves the DMM selectivity and the initial activity of the $H_4SiW_{12}O_{40}/SiO_2$ catalyst.

3.4. Effect of feeding modes for the oxidation of DME to DMM over $MnCl_2$(5 wt%)–$H_4SiW_{12}O_{40}/SiO_2$ catalyst

Table 4 displays the effect of different feeding modes over $MnCl_2$(5 wt%)–$H_4SiW_{12}O_{40}/SiO_2$ catalyst on DME conversion and DMM selectivity. When pure DME reacts with O_2, DMM is the main product and its selectivity reaches 37.5% at 1 h. However, when pure CH_3OH reacts with O_2, only 3.9% of DMM selectivity is obtained, but the selectivity of side-product DME achieves 61.3%. Besides, C_2H_4 and CO selectivities are gained at 11.9%, 12.4%, respectively. At the same time, H_2 is also detected in the gaseous products. Over this catalyst, CH_3OH mainly reacts by dehydration reaction. When H_2O is co-fed with DME and O_2 to the reactor, DMM in product is not found while large amount of CH_3OH (82.1% of selectivity) is yielded, so the hydrolysis reaction becomes the main reaction and inhibits the reaction of DME selective oxidation to DMM. In the synthesis of DMM from the oxidation of DME over $MnCl_2$(5 wt%)–$H_4SiW_{12}O_{40}/SiO_2$ catalyst, except for the formation of DMM from reaction of HCHO with CH_3OH (formed by DME hydrolysis), there maybe exist another route for DMM synthesis from DME selective oxidation directly. DME can absorb on the surface of optimum acid sites and decomposes into methoxy [9], then methoxy can be oxidized on redox sites, therefore, DMM can be synthesized via methoxy under the cooperation of the acid sites and redox sites. Optimum acid sites help DME decompose to methoxy, if the acidity of the catalyst is too strong, methoxy is not easily decomposed and DME may absorb strongly and is over-oxidized to CO_x on the surface of catalyst. $MnCl_2$ addition to $H_4SiW_{12}O_{40}/SiO_2$ moderates the acidity and increases the oxidative activity of the catalyst. DME can be selectively oxidized to DMM over bifunctional catalysts such as $MnCl_2$–$H_4SiW_{12}O_{40}/SiO_2$. The total reaction routes of DME to DMM are proposed in Scheme 1.

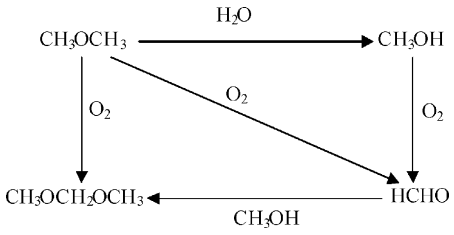

Scheme 1. Total reaction routes of DME to DMM.

3.5. Catalyst characterization

Fig. 2 shows the XRD patterns of $MnCl_2$(5 wt%)–$H_4SiW_{12}O_{40}/SiO_2$ catalyst calcined at different temperatures. At 623 and 673 K, MnO_2 diffraction peaks are found. With the calcined temperatures increases, the diffraction peaks of the catalysts become more and more distinctive. When the temperature exceeds 673 K, the diffraction peak at $2\theta \approx 9^\circ$, which is one of the peaks [10] of the Keggin structure, disappears and the diffraction peaks at $2\theta \approx 23^\circ$, 33° become broader and higher. It can be found that the Keggin structure of the catalysts are destroyed, and WO_3 is released from the catalysts, concurrently $MnWO_4$ is formed when the temperature exceeds 673 K. The changes of the Keggin structure and Mn species of the catalyst maybe result in the catalytic activity decline for the oxidation of DME to DMM when the calcination temperature is above 673 K.

Fig. 3 depicts the XRD patterns of $MnCl_2$ modified $H_4SiW_{12}O_{40}/SiO_2$ catalysts prepared by the different impregnation sequences and the sample after DME oxidation at 593 K ($MnCl_2$(5 wt%) + $H_4SiW_{12}O_{40}$)/SiO_2 diffraction peaks obviously shows broader than the other two at $2\theta \approx 9^\circ$. Besides, the peaks at $2\theta \approx 20.1^\circ$, 28.0° referred to MnO_2 and SiO_2 can be easily found. While diffraction peaks of $H_4SiW_{12}O_{40}$–$MnCl_2$(5 wt%)/SiO_2 show hardly distinctive

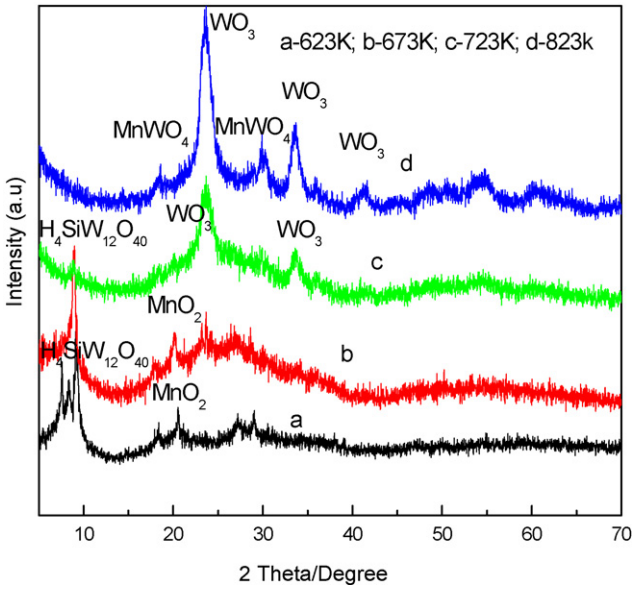

Fig. 2. XRD patterns of $MnCl_2$(5 wt%)–$H_4SiW_{12}O_{40}/SiO_2$ catalyst calcined at different temperatures.

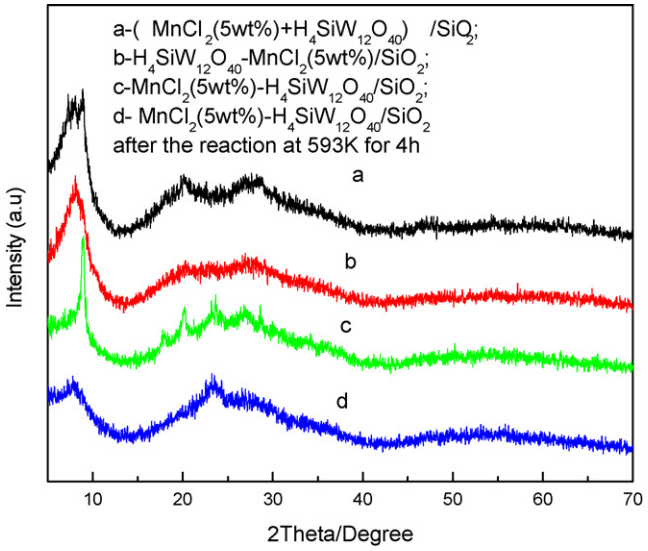

Fig. 3. XRD patterns of the catalysts prepared by different impregnation sequences.

except at $2\theta \approx 9^\circ$ contrasted to the other two samples. Maybe some diffraction peaks of $H_4SiW_{12}O_{40}$ cover the compound including Mn species. In contrast to the fresh sample, the diffraction peak becomes much weaker at $2\theta \approx 9^\circ$ for the sample after the reaction, and the peak at $2\theta \approx 20.1^\circ$ referred to MnO_2 is not easily found.

Fig. 4 shows NH_3-TPD spectra for the samples of $MnCl_2$(5 wt%)–$H_4SiW_{12}O_{40}/SiO_2$ calcined at 623, 673, 723 and 823 K. When the sample is calcined at 623 K, its acidity shows the strongest. With the calcination temperature increased, the acidity becomes weaker and acid site numbers also decrease, concurrently the samples only shows one acid site. It can be found that differences of calcination temperature greatly affect the acidity of the catalysts. Higher calcination

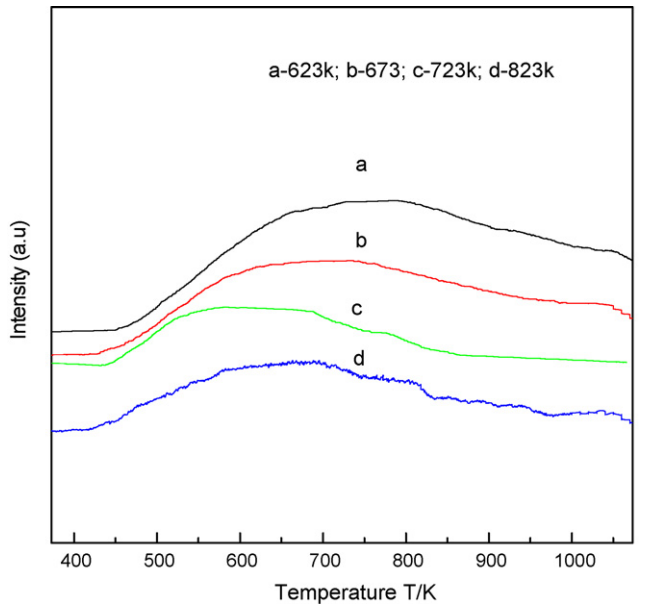

Fig. 4. NH_3-TPD spectra of $MnCl_2$(5 wt%)–$H_4SiW_{12}O_{40}/SiO_2$ prepared at different calcination temperatures: (a) 623 K; (b) 673 K; (c) 723 K; (d) 823 K.

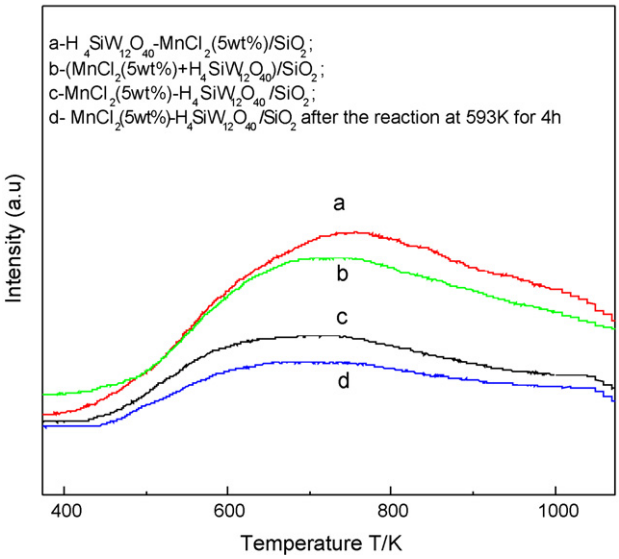

Fig. 5. NH_3-TPD spectra of $MnCl_2$(5 wt%)–$H_4SiW_{12}O_{40}/SiO_2$ prepared by different impregnation sequences and the sample after the reaction.

temperature results in weaker acidity because the Keggin structure of catalysts have been destroyed as can be seen from Fig. 2.

Fig. 5 shows the NH_3-TPD spectra for the samples of $MnCl_2$(5 wt%)–$H_4SiW_{12}O_{40}/SiO_2$ prepared by different impregnation sequences. Obviously, the acid site number is much larger for $H_4SiW_{12}O_{40}$–$MnCl_2$(5 wt%)/SiO_2 with acid site at about 750 K. Then for ($MnCl_2$(5 wt%) + $H_4SiW_{12}O_{40}$)/SiO_2, the acidity is stronger than $MnCl_2$(5 wt%)–$H_4SiW_{12}O_{40}/SiO_2$, but weaker than $H_4SiW_{12}O_{40}$–$MnCl_2$(5 wt%)/SiO_2. It can be found that different impregnation sequences for the catalysts have different effects on their acidity. Therefore, the optimum acidity of the catalyst is very important to the catalytic activity for DME to DMM compared to the results in Table 3. Comparatively, the acidity of the sample after the reaction becomes

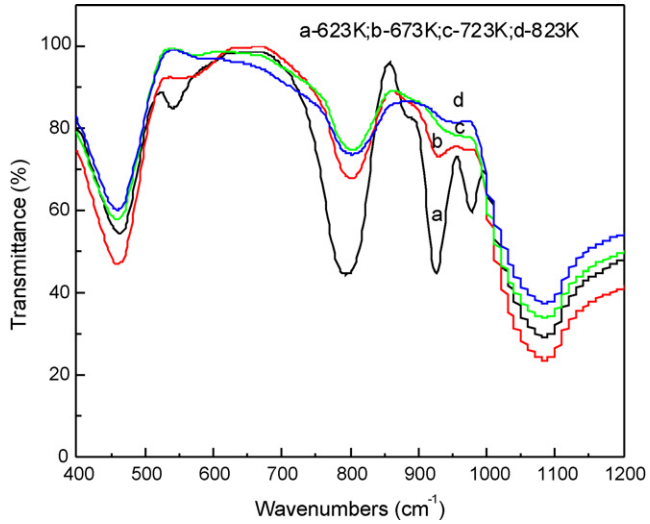

Fig. 6. IR spectra of $MnCl_2$(5 wt%)–$H_4SiW_{12}O_{40}/SiO_2$ calcined at different temperatures.

weaker than that of the fresh $MnCl_2$(5 wt%)–$H_4SiW_{12}O_{40}/SiO_2$ sample, indicating especially some acidic sites disappear.

Fig. 6 shows IR spectra of $MnCl_2$(5 wt%)–$H_4SiW_{12}O_{40}/SiO_2$ catalyst calcined at different temperatures. When the catalyst was calcined at 623 K, the peaks of Keggin structure (Si-Oa 1087.10 cm^{-1}, W-Od 975.31 cm^{-1}, W-Ob-W 925.37 cm^{-1}, W-Oc-W 801.63 cm^{-1}) [11] are found. When the calcination temperature is increased to 673 K, the peaks become weaker, and the peak of W-Od is not distinctive. When the calcination temperature reaches 723 and 823 K, the peaks of W-Od and W-Ob-W which are the typied peaks of Keggin structure and are also the crucial peaks for the activity of the catalysts nearly disappear. It can be concluded that W-Od and W-Ob-W are easily destroyed with the calcination temperature increased.

Fig. 7 indicates IR spectra of $MnCl_2$(5 wt%)–$H_4SiW_{12}O_{40}/SiO_2$ catalyst before and after 4 h reaction. After 4 h reaction, the peaks (W-Oc-W, W-Ob-W and Si-Oa) become weaker and the peak of W-Od is not found.

Fig. 8 shows the Mn 2p XPS spectra of the fresh $MnCl_2$(5 wt%)–$H_4SiW_{12}O_{40}/SiO_2$, and the sample after the catalytic oxidation of DME at 593 K for 4 h. For the fresh sample, the strongest peak at 642.24 eV may be due to Mn $2p_{3/2}$ for MnO_2 and $MnSiO_3$ [12], because the Mn $2p_{3/2}$ of MnO_2 and $MnSiO_3$ are referred to 642.4 eV, 642.3 eV, respectively. Mn $2p_{3/2}$ of MnO_4^- and $MnCl_2$ are referred to 646.8 and 644.2 eV. After the reaction, the intense peak at 642.12 eV may be referred to Mn $2p_{3/2}$ for reduced Mn species. That is to say, some Mn^{4+} species are used to oxidize DME and get electrons themselves in the reaction, therefore they are reduced to Mn^{2+} or Mn^{3+} species during DME catalytic oxidation. This indicates that Mn^{4+} plays extraordinarily important role in the oxidative reaction. Besides, the change of Mn amount on the catalyst surface before and after the reaction is also obtained from XPS results. The Mn amount on the catalyst surface decreases by 15.5% after the catalytic reaction. Simultaneously, the change of total Mn amount in the samples before and after the reaction is also gained by ICP-ACS. The total Mn amount is reduced by 4.9%. Therefore, some active component is wiped off from the catalyst surface. The decrease of Mn species also leads to the catalyst activity decline.

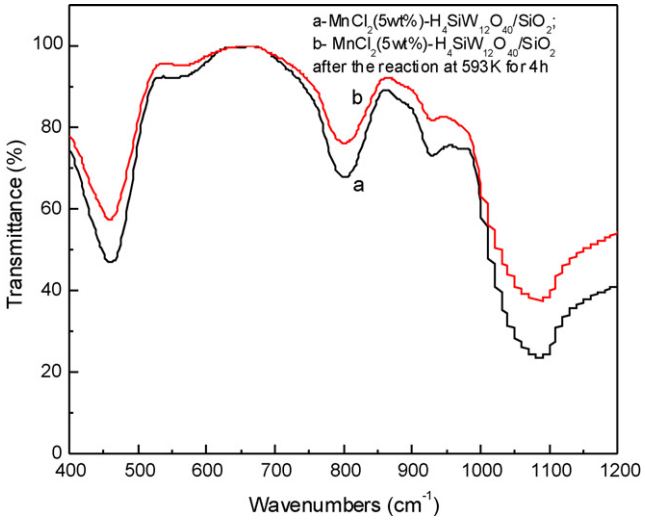

Fig. 7. IR spectra of $MnCl_2$(5 wt%)–$H_4SiW_{12}O_{40}/SiO_2$ catalyst before and after the reaction for 4 h.

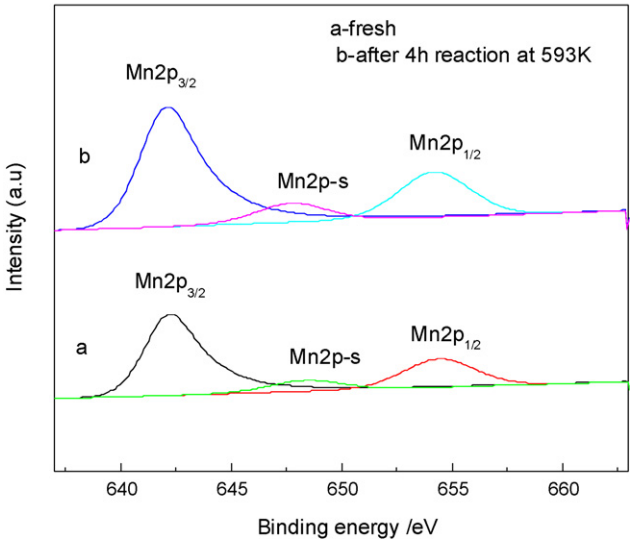

Fig. 8. Mn 2p XPS spectra of $MnCl_2$(5 wt%)–$H_4SiW_{12}O_{40}/SiO_2$.

According to Figs. 2, 4, 6 and 8, the changes of Keggin structure, the changes of Mn species and the decrease of acidity as main reasons result in the activity decline of the sample calcined at 723 K compared to the sample calcined at 673 K, though their BET surface area are similar.

As can be seen from Table 5, the BET surface area decreases from 192.9 to 152.5 m^2/g after 4 h reaction, concurrently total pore volume also drops by 18.5%. But the average pore diameter scarcely changes after the reaction. The structure destroy mentioned previously of the surface particles results in the decrease of BET surface area, and also some Mn particles migration and carbon deposition within the pores lead to the decline of total pore volume, which induces the decrease of the catalytic activity of the catalyst.

Fig. 9 demonstrates the TEM images of $MnCl_2$(5 wt%)–$H_4SiW_{12}O_{40}/SiO_2$ before and after the catalytic oxidation of DME at 593 K. And Fig. 9 also conveys that there exist distinctive differences in the images between the fresh and the used catalysts. The fresh sample looks relatively dispersible while the sample after the reaction shows some agglomeration among the granules in the catalyst surface.

According to the characterization of the catalysts before and after the reaction, the loss of acidic sites, oxidation sites and carbon deposition also lead to the deactivation of the catalyst.

Table 5
Structure properties of $MnCl_2$(5 wt%)–$H_4SiW_{12}O_{40}/SiO_2$ catalysts for the fresh and the used

	The fresh sample	The used sample
BET surface area, A ($m^2\ g^{-1}$)	192.9	152.5
Total pore volume, v ($cm^3\ g^{-1}$)	0.147	0.120
Average pore diameter, d (nm)	3.042	3.137

$d = 4v/A$.

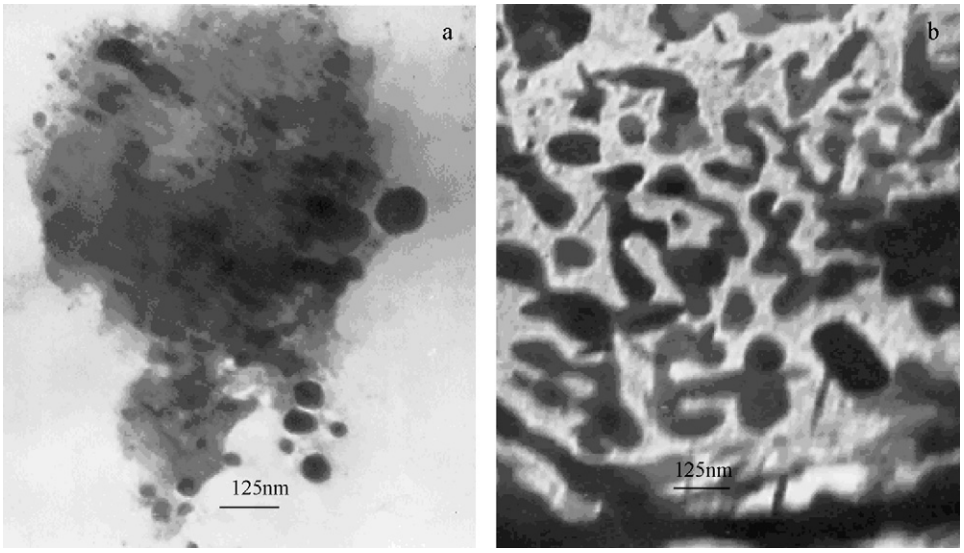

Fig. 9. TEM images of the $MnCl_2$(5 wt%)–$H_4SiW_{12}O_{40}/SiO_2$ catalyst before (a) and after (b) the catalytic DME reaction.

4. Conclusions

In conclusion, the catalytic oxidation of DME to DMM has been successfully conducted over $MnCl_2$ modified $H_4SiW_{12}O_{40}/SiO_2$ catalysts. $MnCl_2$ modification greatly improves the catalytic performance of $H_4SiW_{12}O_{40}/SiO_2$ and obviously increases the DMM selectivity. The catalyst prepared by the sequence of first $H_4SiW_{12}O_{40}$ then $MnCl_2$ ($MnCl_2$(5 wt%)–$H_4SiW_{12}O_{40}/SiO_2$) shows best catalytic activity. The loss of active component happens on the surface of the catalyst. The loss of acidic sites, oxidation sites and carbon deposition also lead to the deactivation of the catalyst.

DMM can be mainly synthesized by DME direct oxidation via methoxy groups formed by DME dissociation under the cooperation of the acid sites and redox sites of $MnCl_2$ modified $H_4SiW_{12}O_{40}/SiO_2$ catalysts at 593 K. There also exists the formation of DMM by reaction of HCHO with CH_3OH (formed by DME hydrolysis).

Acknowledgements

The financial support from the National Natural Science Foundation of China (No. 20373085) and Natural Science Foundation of Shanxi Province (No.20051023) for this study is gratefully acknowledged.

References

[1] SH.J. Wang, K.Y. Tao, J. Liaon. Inst. Technol. 22 (2002) 57.
[2] K.D. Vertin, J.M. Ohi, D.W. Naegeli, et al., Proceedings of the International Spring Fuels and Lubricants Meeting and Exposition, Dearborn, Michigan (USA), May 3–6, 1999, p. 1.
[3] N.V. Pavlenko, Yu.N. Kochkin, N.V. Vlasenko, et al., Teor. Exp. Khim. 36 (2000) 111.
[4] N.V. Vlasenko, Y.N. Kochkin, Russ. J. Appl. Chem. 76 (2003) 1615.
[5] Y.Z. Yuan, H.Ch. Liu, H. Imoto, T. Shido, Y. Iwasawa, J. Catal. 195 (2000) 51.
[6] Y.Z. Yuan, Y. Iwasawa, J. Phys. Chem. B 106 (2002) 4441.
[7] H.Ch. Liu, E. Iglesia, J. Phys. Chem. B 107 (2003) 10840.
[8] Q.D. Zhang, Y.S. Tan, C.H. Yang, Y.Z. Han, Chin. J. Catal., accepted for publication.
[9] O.Y. Feng, Sh.L. Yao, J. Phys. Chem. B 104 (2000) 11253.
[10] Ch.W. Hu, T. Nishimura, T. Okuhara, M. Misono, J. Jpn. Petrol. Inst. 36 (1993) 386.
[11] L.Q. Zhou, Sh.Zh. Liu, Y. Fan, Chin. J. Hubei Univ. (Nat. Sci. Ed.) 24 (2002) 56.
[12] K.Y. Shi, Y.J. Chi, X.Q. Jin, M. Xu, F.L. Yuan, H.G. Fu, Acta Chim. Sin. 63 (2005) 885.